

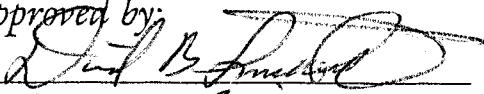
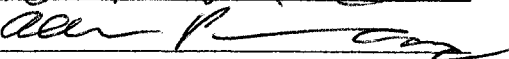
UNIVERSITY OF CINCINNATI

OCT 28, 2002

I, NICHOLAS K. KIM,
hereby submit this as part of the requirements for the degree of:
MASTER OF SCIENCE
in CHEMISTRY

It is entitled THE SYNTHESIS AND INVESTIGATION
OF TEMPLATES CONTAINING A STACKED ARRANGEMENT
OF CARBOXYLATES OVER AROMATIC RINGS.

Approved by:

**The Synthesis and Investigation of Templates Containing a
Stacked Arrangement of Carboxylates over Aromatic Rings.**

A thesis submitted to the

Division of Research and Advance Studies
of the University of Cincinnati

In partial fulfillment of the
requirement for the degree of

MASTER OF SCIENCE

in the Department of Chemistry
of the College of Arts and Sciences

2003

by

Nicholas K. Kim

B.A., Ohio State University, 1992

UMI Number: EP26349

INFORMATION TO USERS

The quality of this reproduction is dependent upon the quality of the copy submitted. Broken or indistinct print, colored or poor quality illustrations and photographs, print bleed-through, substandard margins, and improper alignment can adversely affect reproduction.

In the unlikely event that the author did not send a complete manuscript and there are missing pages, these will be noted. Also, if unauthorized copyright material had to be removed, a note will indicate the deletion.

UMI[®]

UMI Microform EP26349

Copyright 2009 by ProQuest LLC.

All rights reserved. This microform edition is protected against unauthorized copying under Title 17, United States Code.

ProQuest LLC
789 E. Eisenhower Parkway
PO Box 1346
Ann Arbor, MI 48106-1346

ABSTRACT

A salt bridge denotes a pair of oppositely charged groups that form at least one hydrogen bond.¹ In proteins, salt bridges play an important role in structure and function such as in oligomerization, molecular recognition, allosteric regulation, and alpha helix capping. Salt bridges are paired when buried within proteins, but on their surfaces, they are generally exposed to solvent molecules. Stability of salt bridges depends strongly on their environment. Ion transfer from water to protein interiors is a highly unfavorable process,² whereas interactions of ions on protein surfaces have shown to range from being slightly stabilizing to slightly destabilizing.³⁻⁵ Determining the strength of salt bridges within proteins is important for understanding protein properties and for developing novel, artificial receptors capable of binding targeted compounds. Herein, we describe the creation and study of synthetic mimics of a uniquely stacked arrangement of carboxylates over aromatic rings found at protein binding domains and within proteins, which we call *SACA* (Stacked Arrangement of Carboxylates over Aromatic rings). We specifically investigated how the electronic nature of the ring affected salt bridge stability and developed synthetic methodology that allowed these *SACA* templates to be attached to solid supports or other synthetic compounds.

DEDICATION

I like to dedicate this work to my parents who have sacrificed so much to raise us.

Thank you, mom and dad.

ACKNOWLEDGMENT

The author would like to thank Proctor & Gamble Pharmaceutical for generous donation for this project and Dr. X. Eric Hu for much assistance. I also would like to thank Professor David Smithrud for giving me an opportunity to work in his group and for his assistance and patience, and Dr. Allan Pinhas for serving on my committee. And lastly, I would like to thank the University of Cincinnati, Dr. Frank Elbetino, and Dr. Adam Mazur for making this research possible.

TABLE OF CONTENTS

	Pages
TITLE	i
ABSTRACT	ii
DEDICATION	iv
ACKNOWLEDGEMENT	v
TABLE OF CONTENTS	1
LIST OF TABLES	2
LIST OF FIGURES	3
LIST OF SYMBOLS	4
INTRODUCTION	5
RESULTS AND DISCUSSION	11
Template Design	11
Synthesis	12
Binding Study	22
EXPERIMENTAL SECTION	26
Material and Methods	26
Synthetic Procedures	27
Determining Association Constants	38
¹ H NMR Study in D ₂ O	38
¹ H NMR Study in DMSO-d ₆	40
Determining pK _a 's	42
REFERENCES AND NOTES	46

LIST OF TABLES

		Pages
Table 1	Alkylation of alpha-carbon of 25 .	21
Table 2	ΔG° values for arginine with the templates in two solvent systems.	24
Table 3	pK_a values of the templates in H ₂ O and in DMSO.	25
Table 4	Sample preparation table for NMR binding studies in D ₂ O.	39
Table 5	Raw data of arginine chemical shifts in D ₂ O NMR study.	40
Table 6	Sample preparation table for NMR binding studies in DMSO-d ₆ .	41
Table 7	Raw data of arginine chemical shifts in DMSO-d ₆ NMR study.	41
Table 8	pH values in H ₂ O for each template obtained from the potentiometric titrations.	42
Table 9	pH values in DMSO for each template obtained from the potentiometric titrations.	44

LIST OF FIGURES

	Pages	
Figure 1	The X-ray crystallographic structure of the arginine binding sites.	10
Figure 2	Predicted mechanism of indene's isomerization to 2H-indene.	12
Figure 3	Possible route for obtaining a functionalized <i>SACA</i> -template	16
Figure 4	Predicted by-product using mass spectrometry.	18
Figure 5	Reaction intermediate shows the similarity with Danishefsky's diene.	18
Figure 6	A reaction analysis using mass spectrometry.	19

LIST OF SYMBOLS

kcal	Kilocalories	ΔG°	Gibb free energy
mol	Mole	g	Grams
mmol	Millimole	mL	Milliliters
pK_a	$-\log K_A$	eq	Equivalent
K_A	Association constant	μM	Micromole
		μL	Microliter
asp	Aspartic acid	lys	Lysine
asn	Asparagine	pro	Proline
arg	Arginine	ser	Serine
gln	Glutamine	trp	Tryptophan
glu	Glutamic acid	tyr	Tyrosine
gly	Glycine		

INTRODUCTION

Charged groups, which can potentially form salt bridges, exist throughout a protein. Examination of the exterior of 46 monomeric proteins shows that 57% of the residues are non-polar aliphatic or aromatic groups, 24% are polar, and 19% are charged.¹ Less polar side chains are found in the interior of proteins (58% are non-polar aliphatic and aromatic groups, 39% are polar, and 4% are charged). One difference found for interior versus exterior charged groups is that interior ones generally exist as salt bridges, whereas exterior ones generally do not. Salt bridges on protein surfaces are weaker because the ions have a greater mobility and are exposed to an aqueous environment.² Even if paired charges do exist, they do not necessarily contribute to the stability of the protein structure. Interior salt bridges, however, appear to have functionally or structurally important roles.

Determining the strength of salt bridges and their importance in protein properties is difficult because protein structure stems from many weak interactions. Currently, the strength of salt bridges, especially solvent exposed ones, is controversial. Some studies show that external salt bridges contribute 1-2 kcal/mol to protein stability.³ Creating a salt bridge on the surface of T4 lysozyme by incorporating His and Asp residues gave a net stability of 3 kcal/mol when compared to the non-mutated form.⁴ The strength of the Glu2 – Lys10 pair, which exist at the i and $i+4$ position of an

α -helix at the N-terminal end of ribonuclease, is estimated to provide 0.5 kcal/mol of stabilization energy.⁵ The four interior residues, Asp251, Lys178, Arg186, and Asp182 form a ring of four salt bridges in cytochrome P450cam, bind the heme cofactor, and control substrate access to the buried active site.⁶ Glu73 is an important charged residue in the binding site of barnase-barstar. It is located in the active site, contributes to the stability of barnase⁷, and contributes to the binding of barstar.⁸ And lastly, the thermodynamic stability of the N-terminal domain of λ repressor depends on Asp14 forming an intrahelical, hydrogen bond/salt bridge with Ser77 and Arg14, respectively.⁹ These interactions are stabilizing by 0.8 to 1.5 kcal/mol. Asp14, by itself without Ser77 and Arg14, is destabilizing by 0.9 kcal/mol.

Consistent with the confusing nature of salt bridges, for all the cases of favorable salt bridges, there seems to be an equal number of unfavorable ones. Replacing salt bridges within a variant of Arc repressor with hydrophobic residues increased protein stability,¹⁰ and energy estimates of some buried salt bridges using continuum electrostatic calculations¹¹ are unfavorable. Incorporating salt bridges within proteins definitely does not guarantee a favorable energy term. The addition of a salt bridge into an α -helix dimer destabilized it,¹² and a salt bridge incorporated into a surface helix of T4 lysozyme appeared to have little affect on protein stability.^{4B} A salt bridge between Lys6 and Gln14 of hyperthermophilic rubredoxin variant

(PFRD-XC4) does not show any contributions to the stability of the structure.¹³

Solvents affect the strength of a salt bridge. It is known that ionic groups are thermodynamically more stable when immersed in a high-dielectric medium such as water than when embedded in a lower dielectric medium.

Theoretical calculations of a salt bridge in T4 lysozyme (75% buried) showed that its formation during protein folding, where the bridge is transferred from water into the protein interior, destabilizes the protein by 3.5 kcal/mol. On the other hand, the formation of a solvent-exposed salt bridge (37% buried) of uteroglobin was calculated to provide about 1 kcal/mol to protein stabilization.¹⁵ In general, the transfer of a salt bridge from a high-dielectric medium such as water to a lower dielectric medium like an interior of a protein costs about 10 to 16 kcal/mol.¹⁶

Our research goal is to create peptidomimetics of protein binding domains in order to obtain a greater understanding of salt bridges and to obtain compounds that selectively bind protein surfaces. A suitable salt bridge model was observed in the X-ray crystallographic structure of the HyHEL-5 – lysozyme complex (Fig. 1A). Arg68 of lysozyme interacts with the side chains of Glu50, Asn58, and Trp33 of HyHEL-5. The binding domain of HyHEL-5 is highly specific for Arg. Replacing the Arg residue with a Lys reduces the binding affinity by 10^3 .¹⁷ The complex appears to be held together by a salt

bridge, the cation- π interaction, and van der Waals forces. An intriguing feature that has not been discussed in a great detail is the positioning of Glu50 over the electron-rich face of Trp33, in which we refer to as a *SACA*-site (Stacked Arrangement of Carboxylates over Aromatic rings). Having two electron-rich centers in close proximity should be unfavorable. *SACA*-sites were also observed in the human growth hormone receptor (hGHR) (Fig. 1B). In the human growth hormone (hGH), Glu44, Asp164, and Trp169 are interacting with Arg64. These residues from hGHR are considered as a "hot spot" because they provide the majority of the binding energy for the complex.¹⁸ Another *SACA* site was found in a fibrinogen complex (Fig. 1C). Arg3 of the tripeptide (Gly-Pro-Arg) is positioned between the phenol ring of Tyr363 and the two carboxylates of Asp330 and Asp364 of fibrinogen.¹⁹

Traditionally, it is believed that aromatic rings stabilize salt bridges through a combination of a cation- π interaction with Arg, an increase in the site's hydrophobicity, and van der Waals forces. The interaction between cations and aromatic rings is common in proteins. For example, 50% of Arg's are within van der Waals contact distance to an aromatic ring.²⁰ This bond is stabilized by the favorable interaction between a cation and the π electrons of an aromatic ring and van der Waals forces. The guanidinium group of Arg is held directly over the ring in a stacked geometry, which is stabilized by the hydrophobic effect and preferred over a perpendicular geometry.²¹ This configuration leaves the nitrogen atoms of the guanidinium moiety free to

engage in interaction with oppositely charged groups. Having less water around this region also lowers the desolvation penalty for salt bridge formation.³

We have discovered that the placement of an aromatic ring below the carboxylate is necessary for salt bridge formation in water. The purpose of this research is to further explore the role of the aromatic ring in *SACA*-sites in the protein recognition process. Specifically, we examined the relationship between the electron density of an aromatic ring and the strength of the salt bridge with an arginine derivative. Changing the electronic density should both increase the strength of the cation- π interaction and raise the pK_a of the carboxylates. This latter effect has not been invoked for explaining the properties of protein binding sites. Placing a variety of substituents were added to the aromatic ring to alter its electron density. Another goal was to develop *SACA*-site- mimics that can be readily incorporated into a variety of artificial antibodies or receptors.

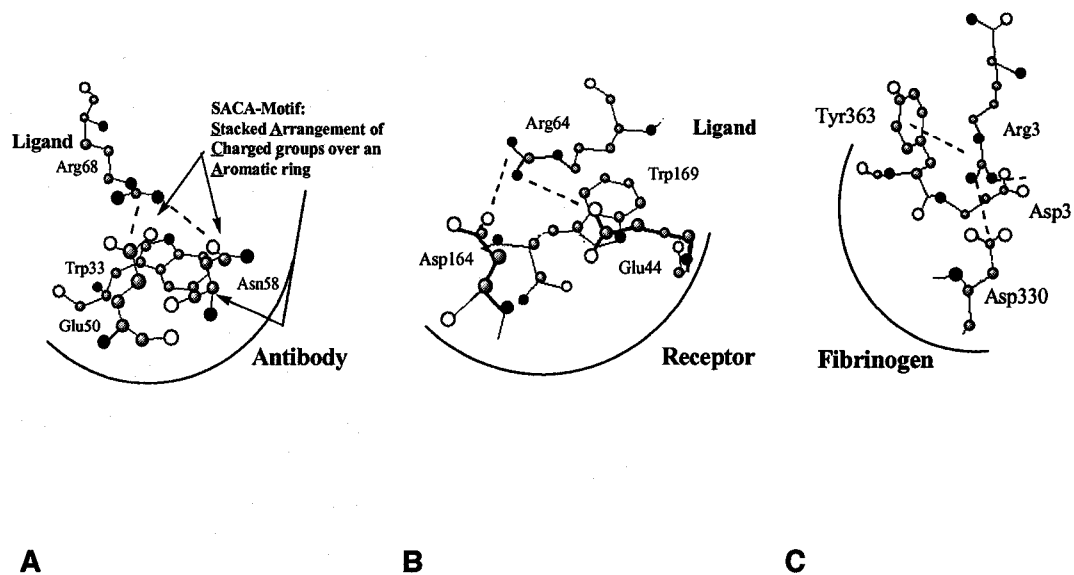
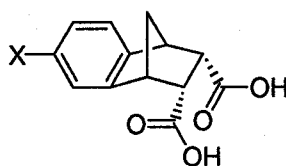


Figure 1. The X-ray crystallographic structures of the arginine binding sites of **A.** HyHEL-5 using Trp33, Asn58, and Glu50 to bind Arg68, **B.** Human growth hormone receptor using Trp169, Glu44, and Asp164 to bind Arg64, and **C.** Tyr363, Asp330, and Asp 364 of fibrinogen binding Arg3. All structures were obtained from the Protein Data Base. The spheres represent the following atoms: white-oxygen, black-nitrogen, and gray-carbon, and the dash line represents a H-bond (arbitrarily drawn).

RESULTS AND DISCUSSION

Template Design

Our first goal was to create a simple synthetic route that produces a variety of aromatically substituted SACA templates. Ideally, the route should produce templates that can be further functionalized to provide attachment sites, allowing the templates to be combined or attached to a solid support. The original targeted templates **1a-d** consisted of the prerequisite dicarboxylic acids for salt bridge formation, an aromatic ring for cation- π interactions, and various substituents on the aromatic ring.



- 1 a** x = H
- b** x = NO₂
- c** x = NH₂
- d** x = OH

The substituents were chosen to give the aromatic ring a wide range of electronic density from the more electron poor nitro (NO₂)substituted ring (template **1b**) to the more electron rich template **1c**, which contains an amine (NH₂)moiety.

Synthesis

The basic scaffold was created based on the work of Huebner²² who demonstrated that indene **2** could undergo a Diels-Alder reaction with maleic anhydride in the presence of hydroquinone, and tetralin (1,2,3,4-tetrahydronaphthalene) to give the bicyclic, anhydride template **3** (Scheme 1). The proposed mechanism has indene undergoing a hydrogen shift and a double bond migration, giving 2*H*-indene (Fig. 2). This intermediate is one of the most reactive Diels-Alder diene, and thus, it is readily captured by maleic anhydride to form the desired product.²³ A role of hydroquinone was not stated but most likely it acts as a radical trap, getting oxidized to 1,4-benzoquinone, reducing the dimerization potential of indene.

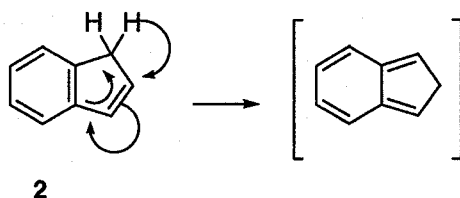
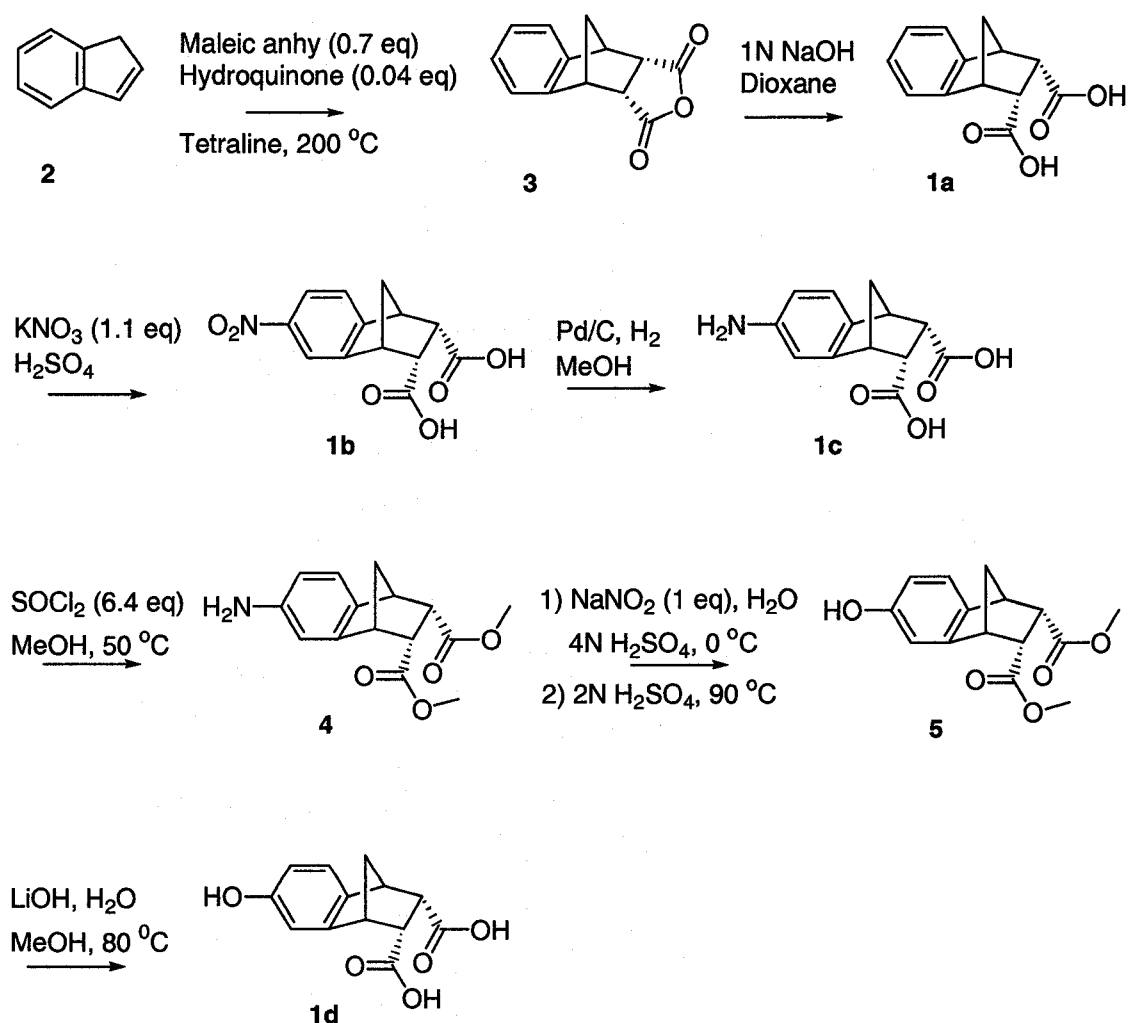


Figure 2. Predicted mechanism of indene's isomerization to 2*H*-indene.

Anhydride **3** was hydrolyzed to the diacid template **1a** using 1*N* sodium hydroxide (NaOH) in dioxane. Less satisfactory results were obtained using 1*N* sodium hydroxide in methanol (MeOH). The rest of the templates were derived sequentially starting with template **1a**. Nitration of the aromatic ring, giving template **1b**, was accomplished upon exposure to potassium nitrate (KNO₃) in sulfuric acid (H₂SO₄) at 0 °C. Direct conversion of the anhydride intermediate **3** to template **1b**, using the same reaction conditions, resulted in

both the mono- and di-nitrated rings, according to mass spectrometric analysis. Attempts to mono-halogenate anhydride **3** with chlorine or bromine atoms were also unsuccessful. The addition of N-chlorosuccinimide²⁴ resulted in mostly unreacted starting material, mono-, and di-chlorinated aromatic rings. Bromination, using benzyltrimethylammonium tribromide,²⁵ gave products that were difficult to identify by thin layer chromatography (TLC) or mass spectrometric analysis.

Scheme 1



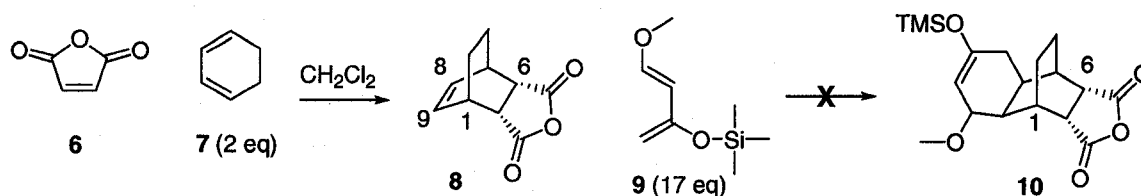
Hydrogenation of nitro template **1b** with palladium on carbon (Pd/C) gave amine **1c**. A direct conversion of amine **1c** to alcohol **1d**, using isoamyl nitrite in dimethylformamide (DMF),²⁶ was attempted without success. Only the starting amine **1c** was retrieved. Esterification of **1c** was performed with thionyl chloride (SOCl₂)²⁷ followed by the addition of MeOH. Attempts to esterify with trimethylsilyl diazomethane (TMSCH₂N₂) produced mainly the mono-, di-, and possibly, the trimethylamine. A substitution reaction of the amine of diester **4** to the alcohol **5** was carried out in sodium nitrite (NaNO₂) / H₂SO₄²⁸. De-esterification of intermediate **5** was performed with lithium hydroxide (LiOH)²⁹ over potassium hydroxide (KOH) to retrieve a cleaner crude material, which after purification gave template **1d**.

Although indene is an ideal starting material to obtain various SACA templates, further derivatization of the templates to provide linker sites would be difficult. Therefore, we attempted to build SACA templates by first adding various functional groups and then aromatizing the template. We also wanted to study the relationship between ring structure and template reactivity. Therefore, an optimal route would allow the construction of templates with different sized aliphatic rings.

The initial route was based on tandem Diels-Alder reactions because they provide multiple functional groups and ring sizes. Maleic anhydride and 1,3-cyclohexadiene were stirred in dichloromethane to obtain anhydride **8** in a 98% yield after purification (Scheme 2). Unfortunately, the second Diels-

Alder reaction using Danishefsky's diene (1-methyl-3-trimethylsiloxy-1,3-butadiene) did not work, even under excessive heating (200 °C) for 24 h. Most likely, Danishefsky's diene is too bulky to react with the dienophile, which exists in a crowded site.

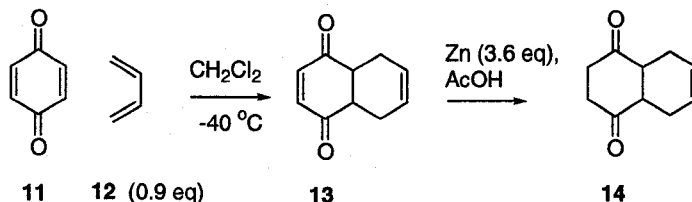
Scheme 2



According to Ghosh,³⁰ the steric hindrance caused by the anhydride portion can be overridden by a favorable electronic effect. This can be accomplished by strategically placing an electron donating group like a hydroxy (OH) or methoxy (OCH₃) group at the C-1 position. To obtain the necessary substituent, quinone was used as the starting dienophile. A Diels-Alder reaction between 1,4-benzoquinone **11** and 1,3-butadiene in dichloromethane yielded 53% of the bicyclic adduct **13** (Scheme 3). Less than 1 equivalent of 1,3-butadiene was used to prevent a second Diels-Alder reaction, and the reaction had to be performed in a high-pressure tube and shaken to maximize the interaction between the reagents. After purification, some unreacted 1,4-benzoquinone was retrieved. Selective reduction of the conjugated double bond was carried out with zinc (Zn) dust in acetic acid (AcOH) to obtain 38% of diketone **14** as crude material. However after

chromatography, the yield was only 3%. This route generally produces a high yield (90%) of diketone **14**.³¹

Scheme 3



We envisaged that compound **14** could be converted into a diene for a subsequent Diels-Alder reactions to give compound **15** by trapping its enolates with trimethylsilyl chloride (TMSCl) under thermodynamic conditions (Fig. 3).³² Unfortunately, the Diels-Alder reaction with crude diene gave only starting alkene **14** and **16**.

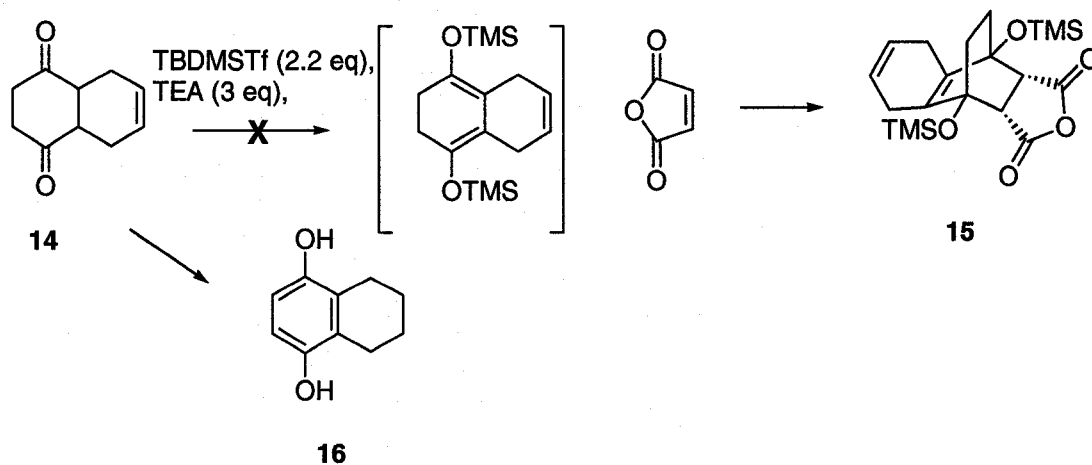
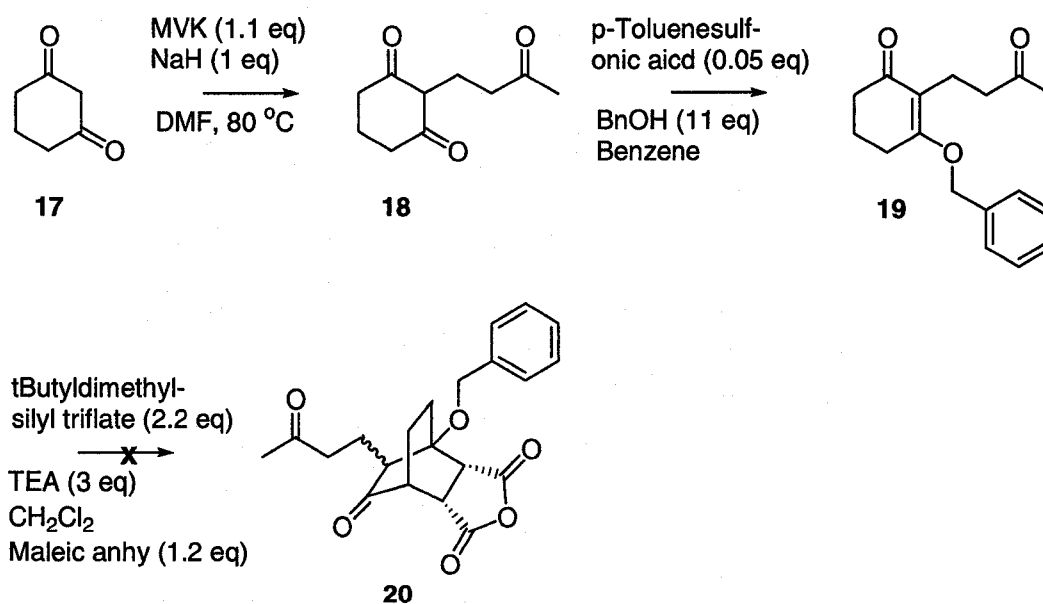


Figure 3. Possible route for obtaining a functionalized SACA template. Template **15** would be aromatized to give the basic template with two linking sites. Unfortunately, it appears that hydroquinone **16** is produced upon enolization.

It is possible that aromatization occurred under the reaction conditions (Fig. 3) to give derivatized hydroquinone **16**. Steric interactions between the bulky trimethylsilyl (TMS) groups and maleic anhydride may be responsible for the poor yields.

A modified method was developed that builds the aromatic ring after the tandem Diels-Alder reactions. The sodium salt of 1,3-cyclohexanedione **17** is reported to undergo a Michael addition reaction with methyl vinyl ketone (MVK) in DMF to give the alkylated diketone **18**.³³ Unfortunately, this reaction gave extensively a mixture of by-products in our hands (Fig. 4). Product purification by vacuum distillation gave decomposition.

Scheme 4



Protected carbonyl, 2-(2-bromoethyl)-2,5,5-trimethyl-1,3-dioxane was chosen as a replacement for MVK to reduce the number of by-products. The reaction rate was very sluggish, and it never went to completion.

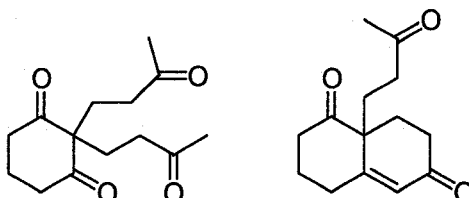


Figure 4. Predicted by-product using mass spectrometry.

In any case, enough product was obtained to continue with the reaction scheme. From this point on, non-purified materials were used to determine if the desired diene **19** could be obtained. Trapping one enolate with benzyl alcohol (BnOH) under acidic conditions followed by TMS trapping of the second resulted in a material that had diene-like properties (Fig. 5). It reacted with maleic anhydride giving an unexpected condensed product (Fig. 6b) instead of the open chain product (Fig. 6a), according to mass spectral analysis.

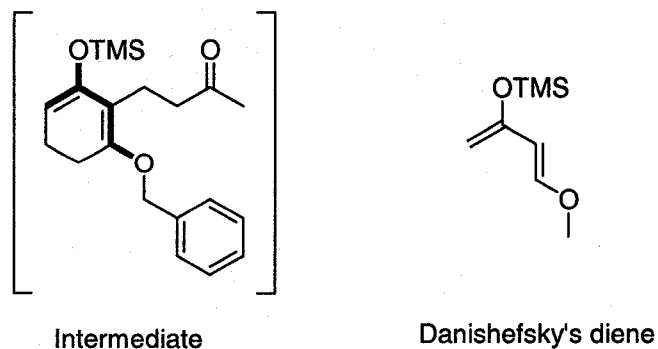


Figure 5. Reaction intermediate shows the similarity with Danishefsky's diene.

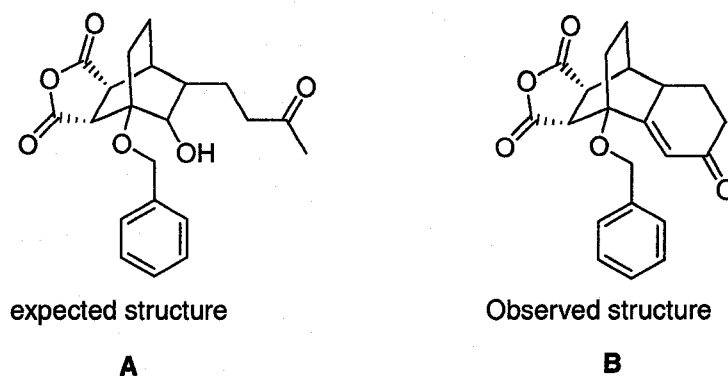
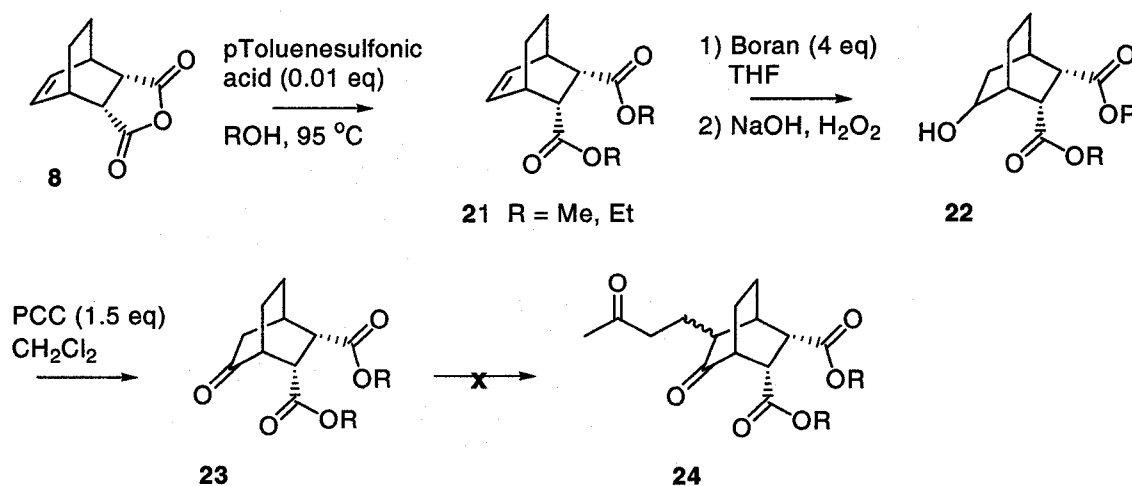


Figure 6. A reaction analysis using mass spectrometry.

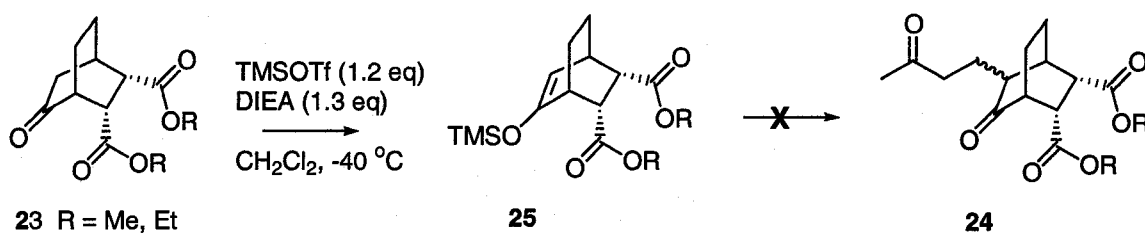
Intermediate **23** was used as a model system to create methods whereby an aromatic ring could be built onto the basic bicyclic scaffold. It was constructed starting from a Diels-Alder reaction between 1,3-cyclohexadiene and maleic anhydride. The anhydride was opened to the dimethyl or diethyl ester under acidic conditions in the appropriate alcoholic solvent. The alkene of compound **21** was converted to the alcohol by hydroboration, and then oxidized to the ketone using pyridinium chlorochromate (PCC). The alcohol generally does not have to be purified prior to oxidation.

Scheme 5



α -Alkylation of ketone **23** proved to be difficult. No product was obtained upon combining ketone **23** with MVK in the presence of triton B in MeOH and heated to 60 °C. Enamine formation was also unsuccessful, but a trapped TMS enolate was obtained. A series of reactions were attempted to alkylate the enol ether under Mukaiyama-type Michael additions reactions.

Scheme 6



These strong Lewis acids [titanium (IV) chloride (TiCl_4), tin (IV) chloride (SnCl_4),³⁴ or titanium (IV) isopropoxide ($\text{Ti}(\text{OiPr})_4$)³⁵] in dichloromethane at -80 °C afforded no reaction and gave only polymerized MVK. The third method used a combination of two catalytic amounts of organometals, zinc (II) chloride (ZnCl_2) and tin (IV) chloride (SnCl_4).³⁶ This method had no effect on **25**. On the other hand, a mild, less acidic Lewis acid, dibutyltin bis(triflate) ($\text{Bu}_2\text{Sn}(\text{OTf})_2$)³⁷ suppressed polymerization of MVK and provided a very small amount of alkylated bicyclic ring **24** by mass spectral analysis.

Table 1. Alkylation of alpha-carbon of **25**

	Conditions	Results
1	TiCl ₄ , Ti(OiPr) ₄ , MVK, CH ₂ Cl ₂ , -80°C	No RX
2	SnCl ₄ , MVK, CH ₂ Cl ₂ , -80°C	No RX
3	SnCl ₄ , ZnCl ₂ , MVK, CH ₂ Cl ₂ , -80°C	No RX
4	1) Bu ₂ Sn(OTf) ₂ , MVK, CH ₂ Cl ₂ , 2) -80°C; 2) 1N HCl	Presence of 24

Binging Study

Association constants were derived for complexes between the SACA templates and N-Ac-Arg-OMe. The concentration of N-Ac-Arg-OMe was held constant, while the concentration of the templates was increased in a stepwise manner. Complex formation causes a change in the magnetic environment of N-Ac-Arg-OMe, producing shifts in the chemical shifts (δ) of its protons. The exchange rate is fast on the nuclear magnetic resonance (NMR) time scale so the chemical shifts reflect an average of the environments of the bound and unbound states. Association constants (K_A) were obtained by comparing the changes in chemical shifts of N-Ac-Arg-OMe with changes in the concentration of the SACA templates. A non-linear least-square fitting procedure was used to solve equation 1⁴², where the difference in the chemical shift ($\Delta\delta$) of an amino acid proton in the presence of template ($\Delta\delta_{\text{obs}}$) and in its absence ($\Delta\delta_0$) depends on the concentration of the template (T), the chemical shift of the proton when it is completely bound to the template ($\Delta\delta_{\text{max}}$), and the association constant of this complex (K_A).

Equation 1.⁴²

$$\Delta\delta = \Delta\delta_{\text{obs}} - \Delta\delta_0 = \frac{K_A [T] \Delta\delta_{\text{max}}}{(1 + K_A [T])}$$

Shifts in the α - and δ - protons of Arg were monitored. The chemical shifts of these protons moved upfield with addition of the template, which is

consistent with the protons becoming shielded by the aromatic ring in the complex.

Examination of K_A 's shows that the degree of association depends strongly on the environment around the complex. The larger K_A 's observed for complexes in methyl sulfoxide- d_6 (DMSO- d_6) compared to deuterium oxide (D_2O) is not surprising. There is a smaller desolvation penalty for salt bridge formation in non-polar solvents, such as DMSO, in comparison to H_2O . The ions, especially anions, associate weakly with DMSO. In water (H_2O), however, both cations and anions interact strongly through H-bonds. These favorable interactions have to be broken before salt bridges can be formed, which detracts from the overall free energy of complexation.

We have already demonstrated that an aromatic ring needs to be placed below the carboxylates to obtain salt bridges in water. A rise in the pK_A 's, caused by the presence of the aromatic ring, is a necessary component of the free energy. The same phenomenon is conserved for the derivatized SACA templates. Higher pK_A 's (Table 3) assures association in water.

A strong correlation was not observed between the electronic properties of the aromatic rings, according to Hammett parameters, and the K_A 's. The lack of correlation might be due to the lack of a resonance interaction³⁸ or a change in the electronic properties.³⁹ It has been noted that the presence of

methylene units in between the aromatic ring and the carboxyl groups can prevent resonance interaction.³⁸ Hydrogen bonds between the hydroxyl hydrogens and water molecules could possibly alter the electronic character of the templates.³⁹

Table 2. ΔG° values for arginine with the templates in two solvent systems.

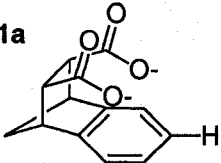
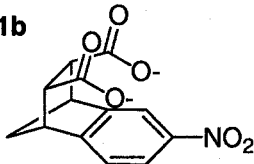
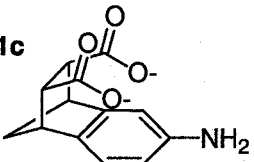
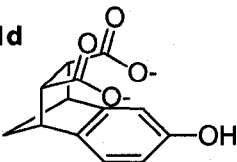
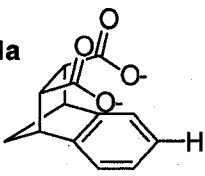
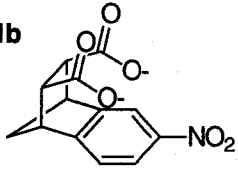
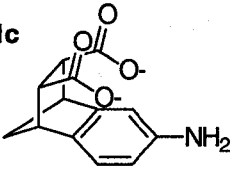
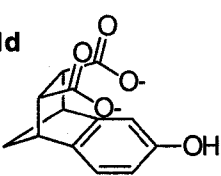
Compounds	N-Ac-Arg-OMe ΔG° (kcal/mol)	
	d_6 -DMSO	D ₂ O
1a 	-3.1 +/- 0.1	-0.57 +/- 0.01
1b 	-2.8 +/- 0.1	-1.39 +/- 0.01
1c 	-2.2 +/- 0.1	-0.35 +/- 0.01
1d 	-2.6 +/- 0.1	-0.63 +/- 0.01

Table 3. pK_A values of the templates in H₂O and in DMSO.

Compounds	Acidity Constants			
	(H ₂ O)		(DMSO)	
	pK_{a1}	pK_{a2}	pK_{a1}	pK_{a2}
1a 	3.89 +/- 0.05	7.40 +/- 0.04	9.2 +/- 0.1	10.58 +/- 0.04
1b 	4.01 +/- 0.05	6.49 +/- 0.04	10.59 +/- 0.07	11.45 +/- 0.06
1c 	3.9 +/- 0.1	7.11 +/- 0.08	8.6 +/- 0.2	10.81 +/- 0.06
1d 	3.85 +/- 0.01	5.01 +/- 0.02	N/A	N/A

EXPERIMENTAL SECTION

Materials and Methods

All solvents and reagents for these reactions were purchased from Aldrich. N-Ac-Arg-OMe was commercially available from CHEM-IMPEX. H₂O and phosphate reagents for the phosphate buffer were purchased from VWR. Proton and carbon nuclear magnetic resonance (¹H and ¹³C NMR) spectra were obtained from a Varian 300 MHz spectrometer equipped with the temperature-control accessory. Chemical shifts are reported in parts per million, and coupling constants are reported in Hertz. Infrared (IR) spectra were taken from Perkin Elmer data station. Low resolution mass spectra (ESI) were processed from micromass ZMD-4000 instrument. The pH values were determined by using pH-MV-meter from VWR. Melting points were measured by Mel-Temp II. High pressure liquid chromatography (HPLC) analysis of compounds was performed by Thermo Separation Products AS3000 using Polaris C18 (3 micron, 4.6 x 25 mm). Absorbance detector was set at 215 and 254 nm wavelength. Prep HPLC for purification of final compounds was done on Rainin Dynamax instrument using Polaris C18 – A (10 micron, 25 x 500 mm). The eluent for both analytical and prep HPLC was gradient using 1% TFA / H₂O and CH₃CN. A flow rate for prep HPLC was set at 60 mL / minute. Analytical silica gel thin layer chromatography (TLC) plates were EM 60 F-254 or Whatman 60 A.

Developed plates were visualized under short wave length UV light. A biotage system was used for chromatography purification.

Synthetic procedures

Endo-1,2,3,4-Tetrahydro-1,4-methanonaphthalene-2,3-dicarboxylic anhydride (3)

A mixture of indene (40 g, 35 mmol), maleic anhydride (24.1 g, 24.0 mmol), hydroquinone (1.5 g) and tetraline (35 mL) were heated at 200 °C for 5 h. The solution was cooled to 120 °C and poured into ethyl acetate (100 mL). This solution, in turn, was poured into toluene (300 mL) with vigorous stirring. ethyl acetate was evaporated under reduced pressure and hot toluene (100 mL) was added to the crude material. The hot toluene mixture was filtered to remove polymer (26 g) and then cooled to -10 °C. The crystalline product was filtered to give 14.14 g (27%) of the anhydride **3**. mp 185-186 °C; (lit.²² mp 181-185 °C); IR (KBr) 3445, 2984, 2945, 1860, 1775 cm⁻¹; ¹H NMR (300 MHz, CDCl₃) δ 7.27 (m, 4H), 3.94 (app s, 2H), 3.82 (app s, 2H), 2.08 (AB quartet, J=9.6, 1.5 Hz, 2H); ¹³C NMR (75 MHz, CDCl₃) δ 170.82, 141.70, 128.36, 123.34, 52.87, 48.99, 47.53; mass spectrum (ESI), *m/e* 215 (M+1).

Endo-1,2,3,4-Tetrahydro-1,4-methanonaphthalene-2,3-dicarboxylic acid (1a)

To a solution of *Endo-1,2,3,4-Tetrahydro-1,4-methanonaphthalene-2,3-dicarboxylic anhydride* (6.61 g, 30.9 mmol) dissolved in dioxane (165 mL) was added 1N sodium hydroxide (60 mL). The reaction mixture was stirred

for 3 h, poured into a separatory funnel containing ethyl acetate (200 mL) and 1N hydrogen chloride (200 mL), and extracted. After additional extraction with ethyl acetate (2 x), the organic layers were combined, washed with brine (1 x), dried over anhydrous sodium sulfate, and the solvent was removed under reduced pressure. The crude material was suspended in ether and stirred for 24 h to remove excess dioxane. After rinsing the product with fresh ether, diacid **1a** was obtained as a pure white solid 4.94 g, (69%), according to ^1H NMR analysis. mp 177 – 178 °C; IR (KBr) 3186, 2648, 1731, 1720 cm^{-1} ; ^1H NMR (300 MHz, CD_3OD) δ 7.24 (q, $J=5.1$, 3 Hz, 2H), 7.05 (q, $J=5.7$, 3 Hz, 2H), 3.58 (app s, 2H), 3.53 (app s, 2H), 1.81 (dd, $J=16.8$, 7.5 Hz, 2H); ^{13}C NMR (75 MHz, CD_3OD) δ 174.15, 144.59, 125.60, 123.07, 49.73, 47.88, 47.78; mass spectrum (ESI), m/e 233 ($M+1$), 215 ($M+H-H_2O$); HPLC analysis - 96% pure.

Endo-6-nitro-1,2,3,4-tetrahydro-1,4-methanonaphthalene-2,3-dicarboxylic acid (1b)

Endo-1,2,3,4-tetrahydro-1,4-methano-naphthalene-2,3-dicarboxylic acid (6.87 g, 29.6 mmol) was dissolved in a solution of sulfuric acid (33 mL), and potassium nitrate (2.99 g, 29.6 mmol) was added in 3 portions at 0 °C. The reaction mixture was stirred for 1 h at 0 °C, and then warmed to room temperature. Ice was added to the solution, which was stirred for an additional 1 h before filtration. Cold water was used to rinse away excess acid. The solid residue was suspended in ether and stirred for 24 h.

Filtration of the mixture afforded 4.75 g (57%) of the product as a pale yellow solid: mp 155 – 157 °C; IR (KBr) 3390, 3093, 3000, 2615, 2532, 1720 cm^{-1} ; ^1H NMR (300 MHz, CD_3OD) δ 8.11 (app s, 1H), 8.02 (d, $J=7.8$ Hz, 1H), 7.46 (d, $J=8.1$ Hz, 1H), 3.73 (app s, 2H), 3.63 (app s, 2H), 3.36 (s, 2H), 1.92 (AB quartet, $J=9.6, 1.5$ Hz, 2H); ^{13}C NMR (75 MHz, CD_3OD) δ 173.73, 173.56, 152.85, 146.82, 146.70, 123.94, 121.55, 118.41, 49.52, 48.69, 47.85, 47.68, 47.60, 47.44; mass spectrum (ESI), m/e 278 (M+1), 260 (M+H-H₂O); HPLC analysis - 96% pure.

Endo-6-Amino-1,2,3,4-tetrahydro-1,4-methanonaphthalene-2,3-dicarboxylic acid (1c)

Hydrogen gas at ca. 1 atm pressure was applied to a mixture of *endo-6-nitro-1,2,3,4-tetrahydro-1,4-methano-naphthalene-2,3-dicarboxylic acid* (3.99 g, 14.0 mmol), palladium on carbon (20% by wt.), and methanol (200 mL). The reaction mixture was stirred for 2 h and then filtered through celite. The filtrate was evaporated under reduced pressure to yield 3.33 g (94%) of the product as a pale yellow solid: mp > 200 °C; IR (KBr) 3390, 3148, 2983, 2604, 1711, 1687, 1648 cm^{-1} ; ^1H NMR (300 MHz, CD_3OD) δ 7.36 (d, $J=7.8$ Hz, 1H), 7.30 (app s, 1H), 7.07 (d, $J=7.8$ Hz, 1H), 3.65 (s, 2H), 3.60 (dd, $J=8.4, 3.3$ Hz, 2H), 3.37 (s, 2H), 1.87 (AB quartet, $J=20.7, 9$ Hz, 2H); ^{13}C NMR (75 MHz, CD_3OD) δ 173.92, 173.67, 147.32, 145.95, 128.48, 124.28, 119.98, 118.28, 49.78, 48.69, 47.64, 47.42; mass spectrum (ESI), m/e 248 (M+1), 230 (M+H-H₂O), 495 (M+M+H).

Endo-7-Amino-3-formyl-1,2,3,4-tetrahydro-1,4-methanonaphthalene-2,3-dicarboxylic acid methyl ester (4)

To a cooled solution of thionyl chloride (0.78 mL, 10.7 mmol) in 15 mL of methanol (-10 °C) was slowly added. A solution of *endo-6-Amino-1,2,3,4-tetrahydro-1,4-methano-naphthalene-2,3-dicarboxylic acid* (0.41 g, 1.6 mmol) dissolved in methanol (5 mL). The reaction flask was removed from the -10 °C bath and placed in a 50 °C bath. According to TLC analysis, the reaction was completed in 0.5 h. (at 25 °C, the reaction requires 2 h. for completion). The solvent was evaporated under reduced pressure, and the residue was subjected to chromatography using methanol-dichloromethane (1:20) as the eluent. Purification resulted in the isolation of 0.11 g (24%) of the product as a pale yellow oil: ¹H NMR (300 MHz, CD₃OD) δ 7.01 (d, J=8.1 Hz, 1H), 6.67 (d, J=1.8 Hz, 1H), 6.44 (dd, J=7.8, 2.1 Hz, 1H), 3.53 (t, J=1.2 Hz, 2H), 3.51 (s, 3H), 3.50 (s, 3H), 3.43 (t, J=1.2 Hz, 2H), 1.75 (td, J=39.3, 10.8, 1.8 Hz, 2H); mass spectrum (ESI), *m/e* 276 (M+1), 551 (M+M+H).

Endo-3-Formyl-7-hydroxy-1,2,3,4-tetrahydro-1,4-methanonaphthalene-2,3-dicarboxylic acid methyl ester(5)

To a solution of crude *endo-7-amino-3-formyl-1,2,3,4-tetrahydro-1,4-methano-naphthalene-2,3-dicarboxylic acid methyl ester* (1.69 g, 6.14 mmol) in 4 N sulfuric acid (26 mL) at 0 °C was added a solution of sodium nitrite (0.42 g, 6.14 mmol) in water (1 mL). In turn, this solution was added to 2 N

sulfuric acid (20 mL) and the reaction mixture was refluxed for 0.5 h. After cooling to 25 °C, the mixture was extracted with ethyl acetate (3x). The combined organic layers were washed with water (2x) and brine (1x), and then dried over anhydrous magnesium sulfate. After removing solvent under reduced pressure, chromatography was performed with ethyl acetate-hexanes (1:3) to obtain 0.70 g (41%) of the product as a pale red solid. ¹H NMR (300 MHz, CD₃OD) δ 7.02 (d, J=8.1 Hz, 1H), 6.73 (d, J=2.7 Hz, 1H), 6.51 (dd, J=8.1, 2.1 Hz, 1H), 3.54-3.47 (m, 10H), 1.80 (m, 2H).

Endo-6-Hydroxy-1,2,3,4-tetrahydro-1,4-methanonaphthalene-2,3-dicarboxylic acid (1d)

A solution of lithium hydroxide (0.14 g, 5.7 mmol) in water (1.5 mL) was added to a solution of 3-endo-formyl-7-hydroxy-1,2,3,4-tetrahydro-1,4-methano-naphthalene-2,3-dicarboxylic acid methyl ester (0.63 g, 2.2 mmol) in methanol (15 mL). The reaction mixture was refluxed for 24 h. After cooling to room temperature, water (10 mL) was added to the solution. The aqueous layer was washed with ethyl acetate (2x) and then collected. Its pH was adjusted to 2 with the addition of 6 N hydrogen chloride. The aqueous layer was rewashed with ethyl acetate (3x). The combined organic layers were rinsed with brine (1x) and dried over anhydrous magnesium sulfate. A purification was done with prep HPLC, which yield 0.26 g (45%) of the product as a pale yellow solid. IR (KBr) 3208, 2983, 2609, 1706, 1618 cm⁻¹;

mass spectrum (ESI), m/e 247 (M-1), 249 (M+1), 231 (M+H-H₂O), 514 (M+M+NH₄); HPLC analysis - 92% pure.

Endo-4-Oxa-tricyclo[5.2.2.0^{2,6}] undec-8-ene-3,5-dione (8)

To a solution of maleic anhydride (15 g, 0.15 mol) in dichloromethane (300 mL) was slowly added 1,3-cyclohexadiene (33 mL, 0.49 mol). The reaction mixture was stirred for 24 h, and then concentrated to dryness. To the resulting white residue, ether (100 mL) was added and the mixture was stirred for 15 minutes. The mixture was filtered, and the filtrate was concentrated to dryness. Repeating the ether purification procedure resulted in 25.1 g (99% yield) of the product as a white solid. ¹H NMR (300 MHz, CD₃OD) δ 6.33 (dd, J=4.5, 3.3 Hz, 2H), 3.24 (s, 2H), 3.15 (app s, 2H), 1.61 (m, 2H), 1.42 (m, 2H); ¹³C NMR (75 MHz, CD₃OD) δ 173.09, 134.27, 132.28, 45.00, 31.86, 23.19.

4a,5,8,8a-Tetrahydro-[1,4]naphthoquinone (13)

To a solution of 1,4-benzoquinone (8 g, 0.07 mol) in anhydrous dichloromethane (25 mL) at -40 °C was added 1,3-butadiene (3.8 g, 0.070 mol). The flask was shook for 24 h at 25 °C. Evaporation of solvent left 6.3 g (53%) of crude material as a dark green solid. ¹H NMR (300 MHz, CD₃OD) δ 6.68 (s, 2H), 5.69 (s, 2H), 3.25 (t, J=6.3 Hz, 2H), 2.33 (AB quartet, J=87.3, 15.9 Hz, 4H); ¹³C NMR (75 MHz, CD₃OD) δ 187.47, 139.53, 124.63, 46.50, 24.37.

2,3,4a,5,8,8a-Hexahydro-[1,4]naphthoquinone (14)

To a solution of 4a,5,8,8a-tetrahydro-[1,4]naphthoquinone (2.0 g, 0.012 mol) in acetic acid (16 mL) was added zinc dust (2.9 g, 0.044 mol) in three portions. The reaction was stirred for 2 h at 70 °C, cooled to 25 °C, and then filtered. After concentrating the filtrate solution to about 5 mL, and water (15 mL) was added. The aqueous layer was washed with ether (3x). The combined organic layers were washed with water (2x), 1 N sodium hydroxide, and brine. After drying the combined organic layers over sodium sulfate, the crude material was purified by column chromatography with ethyl acetate-Hexanes (1:10) as the eluent. 0.06 g (3%) of the product was obtained as a solid. ¹H NMR (300 MHz, CD₃OD) δ 5.69 (s, 2H), 3.08 (m, 2H), 2.92-2.66 (m, 4H), 2.30 (AB quartet, J=48.9, 15.3 Hz, 4H); ¹³C NMR (75 MHz, CD₃OD) δ 209.47, 124.69, 45.145, 36.11, 23.78.

2-(3-Oxo-butyl)-cyclohexane-1,3-dione (18)

A solution of 1,2-cyclohexanedione (10 g, 89 mmol) in anhydrous dimethylformamide (100 mL) was slowly added to a 0 °C mixture of 60 % sodium hydride (2.14 g, 89.1 mmol) in anhydrous dimethylformamide (300 mL). A solution of methyl vinyl ketone (8.1 g, 98 mmol) in anhydrous dimethylformamide (100 mL) was added to the mixture, which was subsequently stirred for 2 h at 80 °C. The reaction was quenched with 1N hydrogen chloride and extracted with ethyl acetate (3x). After combining the

organic layers, they were washed with satd. Sodium bicarbonate and brine, and then dried over sodium sulfate. Purification was not performed on the crude material.

3-benzyloxy-2-(3-oxo-butyl)-cyclohexanone (19)

To a solution of 2-(3-oxo-butyl)-cyclohexane-1,3-dione (2.0 g, 7.0 mmol) in anhydrous benzene (30 mL) was added p-toluenesulfonic acid (0.12 g, 0.35 mmol) and benzyl alcohol (8.45 mL, 81.6 mmol). A Dean-Stark trap was attached, and the reaction was refluxed for 2 h. When the reaction was completed, the solution was poured into a separatory funnel containing satd. Sodium bicarbonate. Ether was added to the funnel, and aqueous work up was performed with aq. Sodium carbonate (1x), water (1x), and brine (1x). The organic layers were collected and dried over magnesium sulfate. Chromatography with ethyl acetate-hexanes (1:10) yielded 6.9 g of a possible product. IR and NMR data showed the presence of benzyl alcohol.

***Endo*-bicyclo[2.2.2]oct-5-ene-2,3-dicarboxylic acid diethyl ester (21)**

Para-toluenesulfonic acid (0.10 g, 0.55 mmol) was added to a solution of *endo*-4-oxa-tricyclo[5.2.2.0^{2,6}] undec-8-ene-3,5-dione (10 g, 61 mmol) and ethanol (23 mL). The reaction mixture was refluxed for 24 h. After removing solvent under reduced pressure, product was purified by chromatography with ethyl acetate-hexanes (1:15) as the eluent. 10.1 g (69% yield) of the product was obtained as a clear oil. ¹H NMR (300 MHz, CD₃OD) δ 6.32 (ddd, J=4.8, 3, 1.8 Hz, 2H), 4.04 (m, 4H), 3.00 (s, 2H), 2.90 (s, 2H), 1.43 (AB

quartet, $J=71.1, 7.2$ Hz, 4H), 1.20 (dt, $J=8.7, 7.2, 1.8$ Hz 6H); ^{13}C NMR (75 MHz, CD_3OD) δ 173.14, 132.51, 60.48, 47.84, 32.73, 24.80, 14.35; HPLC analysis - 96% pure.

Endo-bicyclo[2.2.2]oct-5-ene-2,3-dicarboxylic acid dimethyl ester (21)

The same procedure to make *endo*-bicyclo[2.2.2]oct-5-ene-2,3-dicarboxylic acid diethyl ester was followed, except methanol was used as the solvent.

The reaction yielded 12.6 g (62%) of product as a white solid. ^1H NMR (300 MHz, CD_3OD) δ 6.31 (q, $J=3.3$ Hz, 2H), 3.58 (s, 6H), 3.01 (s, 2H), 2.88 (bs, 2H), 1.54 (dd, $J=7.5, 1.5$ Hz, 2H), 1.30 (dd, $J=7.8, 1.8$ Hz, 2H); ^{13}C NMR (75 MHz, CD_3OD) δ 173.64, 132.53, 51.78, 47.71, 32.64, 24.72.

Endo-bicyclo[2.2.1]hept-5-ene-2,3-dicarboxylic acid dimethyl ester (21)

The same procedure used to make bicyclo[2.2.2]oct-5-ene-2,3-dicarboxylic acid diethyl (or dimethyl) ester was followed, except methanol and 4-oxatricyclo[5.2.1.0^{2,6}]dec-8-ene-3,5-dione (from Aldrich) were used. The

reaction yielded 21.1 g (66%) of the product. ^1H NMR (300 MHz, CD_3OD) δ 6.25 (t, $J=1.8$ Hz, 2H), 3.59 (s, 6H), 3.28 (t, $J=3, 1.5$ Hz, 2H), 3.15 (q, $J=1.5$ Hz, 2H), 1.39 (AB quartet, $J=42.6, 8.4$ Hz, 2H); ^{13}C NMR (75 MHz, CD_3OD) δ 173.15, 135.14, 51.75, 48.91, 48.27, 46.47; mass spectrum (ESI), m/e 211 (M+1).

***Endo*-5-hydroxy-bicyclo[2.2.2]oct-5-ene-2,3-dicarboxylic acid dimethyl ester (22)**

Borane, as 1 M solution in tetrahydrofuran (11.4 mL, 11.4 mmol), was added to a solution of *endo*-bicyclo[2.2.2]oct-5-ene-2,3-dicarboxylic acid dimethyl ester (0.64 g, 2.8 mmol) in anhydrous tetrahydrofuran (27 mL). The reaction mixture was stirred for 24 h. Additional borane (5.0 mL) was added and the solution was stirred for another 4 h. Water (2 mL), 3M sodium hydroxide (10 mL), and 30% hydrogen peroxide (10 mL) were added, sequentially. The solution was stirred for 1 h, before partitioning it between ethyl acetate and brine. The organic layer was dried over sodium sulfate and concentrated to dryness. The material was purified by chromatography with ethyl acetate-Hexanes (1:4) as the eluent to obtain 0.64 g (92%) of the product. ¹H NMR (300 MHz, CD₃OD) δ 9.18 (bs, 1H), 4.36 (m, 1H), 3.63 (d, J=3.9 Hz, 6H), 2.99 (d, J=3 Hz, 1H), 2.86 (d, J=11.1 Hz, 2H), 2.15-2.01 (m, 3H), 1.71 (t, J=13.2, 1H), 1.46 (t, J=3.6, 1H), 1.28 (m, 3H); ¹³C NMR (75 MHz, CD₃OD) δ 174.48, 174.40, 65.01, 52.11, 51.97, 44.41, 42.91, 33.32, 32.45, 29.23, 25.68, 18.19.

***Endo*-5-hydroxy-bicyclo[2.2.2]oct-5-ene-2,3-dicarboxylic acid diethyl ester (22)**

The same procedure used to make *endo*-5-Hydroxy-bicyclo[2.2.2]oct-5-ene-2,3-dicarboxylic acid dimethyl ester was followed, except *endo*-

bicyclo[2.2.2]oct-5-ene-2,3-dicarboxylic acid diethyl ester was used as the starting material. No characterization was performed.

Endo-5-oxa-bicyclo[2.2.2]oct-5-ene-2,3-dicarboxylic acid dimethyl ester (23)

To a mixture of pyridium chlorochromate (0.80 g, 3.7 mmol) and anhydrous dichloromethane (15 mL) was added a solution of *endo*-5-hydroxy-bicyclo[2.2.2]oct-5-ene-2,3-dicarboxylic acid dimethyl ester (0.60 g, 2.5 mmol) in anhydrous dichloromethane (10 mL). Chromatography of the material with ethyl acetate-Hexanes (1:4) gave 0.46 g (78%) of the product as a clear oil. ^1H NMR (300 MHz, CD_3OD) δ 3.63 (d, $J=4.5$ Hz, 6H), 3.32 (dd, $J=11.4, 3$ Hz, 1H), 3.02 (dt, $J=4.2, 2.4$ Hz, 1H), 2.86 (dt, $J=5.7, 2.7$ Hz, 1H), 2.58 (AB quartet, $J=5.1, 3$ Hz, 1H), 2.53 (AB quartet, $J=6, 3$ Hz, 1H), 2.20 (dt, $J=5.4, 2.7$ Hz, 1H), 1.91-1.82 (m, 2H), 1.73-1.62 (m, 2H); ^{13}C NMR (75 MHz, CD_3OD) δ 213.09, 173.32, 172.66, 52.42, 52.05, 45.55, 45.45, 43.00, 41.46, 29.74, 25.12, 23.23; mass spectrum (ESI), m/e 241 ($M+1$), 258 ($M+\text{NH}_4^+$).

Endo-5-trimethylsilyloxy-bicyclo[2.2.2]oct-5-ene-2,3-dicarboxylic acid dimethyl ester (25)

Trimethylsilane triflate (0.20 mL, 1.1 mmol) was added at -40 °C to a solution of *endo*-5-oxa-bicyclo[2.2.2]oct-5-ene-2,3-dicarboxylic acid dimethyl ester (0.22 g, 0.95 mmol), diisopropylethylamine (0.21 mL, 1.2 mmol) and

anhydrous dichloromethane (3.3 mL). When the addition was done, the reaction was allowed to warm to 25 °C and stirred for 2 h at 25 °C. 1N sodium hydroxide (0.17 mL) was added, while stirring was very vigorous. Hexanes (20 mL) was added and the mixture was stored at -4 °C for 24 h. The mixture was filtered, and the filtrate concentrated to dryness. The oily material was diluted with hexanes (20 mL) and refiltered. After concentrating the material, the product was obtained as a pale yellow solid.

Determining Association Constants

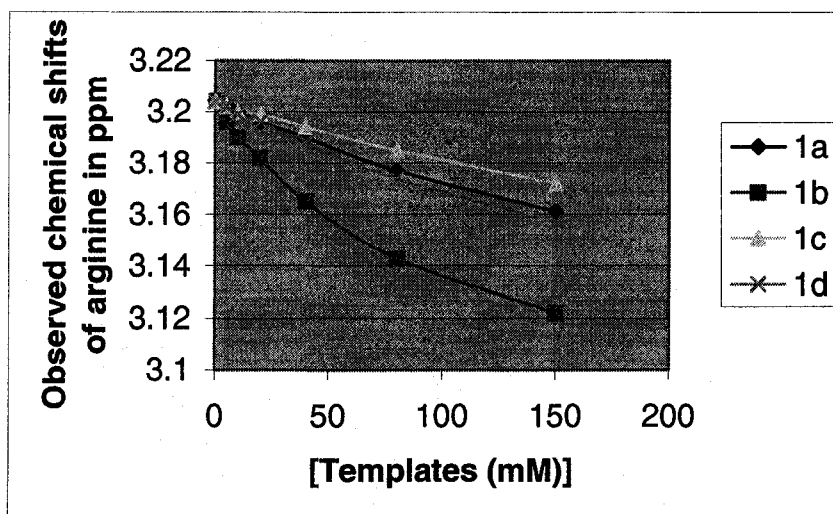
Changes in the chemical shifts of N-Ac-Arg-OMe in D₂O or DMSO-d₆ at 25 °C, caused by the addition of a known quantity of template, were monitored. Association constants were obtained by performing a nonlinear least square fitting procedure of the data. Solutions in D₂O and in DMSO-d₆ were prepared according to the following methods.

H¹ NMR study in D₂O : A phosphate buffer⁴⁰ was prepared by mixing 16 mL of 0.1 M NaH₂PO₄ and 84 mL of 0.1 M Na₂HPO₄, giving a pH 7.5 by a pH meter. Chemical shifts were compared to 2,2-dimethyl-2-silapentane-5-sulphonate (DDS) as the internal standard in D₂O. Stock solutions of the templates (0.15 M) were prepared by dissolving a template and sodium bicarbonate (2 eq) in methanol. The solvent was evaporated under vacuum and left under high vacuum for 24 h. The dried templates were dissolved in

0.8 mL of phosphate buffer. A *N*-Ac-Arg-OMe stock solution (0.25 M) was made by dissolving 0.005 g of the amino acid in 0.8 mL of D₂O. Aliquots of the template, *N*-Ac-Arg-OMe, and buffer solutions were mixed together to give a total volume of 0.400 mL, according to the amounts given in Table 4. For binding studies in D₂O, the chemical shift of *N*-Ac-Arg-OMe's methylene at 3.2 ppm was monitored. *N*-Ac-Arg-OMe's α -proton signal was obscured by the water peak at 4.8 ppm.

Table 4. Sample preparation table for NMR binding studies in D₂O.

Run	Template (mM)	Temp. Vol. (uL)	Arg. Vol. (uL)	Buffer Vol. (uL)
1	0	0	40	360
2	5	12	40	348
3	10	23	40	337
4	20	46	40	314
5	40	93	40	267
6	80	186	40	174
7	150	360	40	0

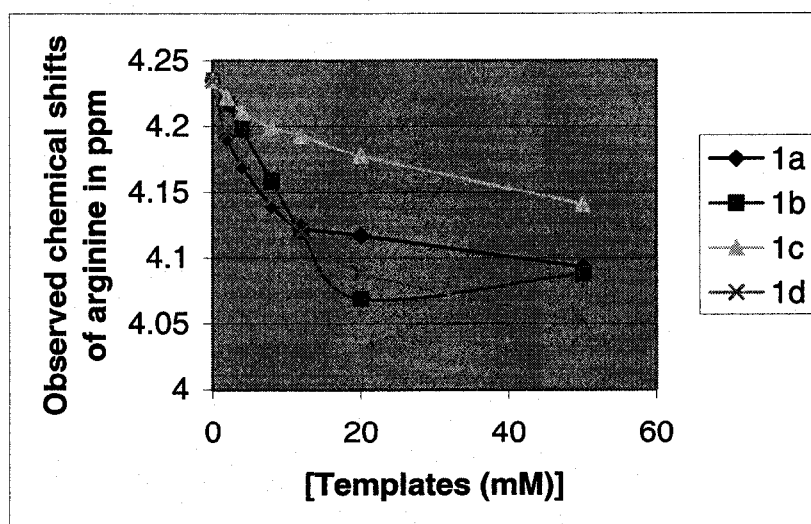
Table 5. Raw data of arginine chemical shifts in D₂O NMR study.

H¹ NMR study in DMSO-d₆: Stock solutions of the templates (0.15 M) were prepared by dissolving a template and tetramethylammonium hydroxide (2 eq) in methanol. Solvent was evaporated under vacuum, and the material was left under high vacuum for 24 h. The dried templates were dissolved in 0.5 mL of DMSO-d₆. A *N*-Ac-Arg-OMe stock solution (0.08 M) was made by dissolving 0.011 g of the *N*-Ac-Arg-OMe in 0.5 mL of DMSO-d₆. Aliquots of the template, *N*-Ac-Arg-OMe, and buffer solutions were mixed together to give a total volume of 400 mL, according to the amounts given in Table 6.

Table 6. Sample preparation table for NMR binding studies in DMSO-d₆.

Runs	Template (mM)	Temp. Vol. (uL)	Arg. Vol. (uL)	DMSO-d ₆ Vol. (uL)
1	0	0	50	350
2	2	8	50	342
3	4	16	50	334
4	8	32	50	318
5	12	48	50	302
6	20	80	50	270
7	50	200	50	150

For DMSO-d₆ binding study, the chemical shift at 4.2 ppm was monitored because the peak around 3.2 ppm gradually overlaps with the signal for DMSO as the concentration of the templates is increased.

Table 7. Raw data of arginine chemical shifts in DMSO-d₆ NMR study.

Determining pK_a 's

Potentiometric titrations: Template solutions (5 mM) were made from boiled, purified water (Millipore). Potentiometric titrations were performed at 25 °C with a 0.105 M solution of NaOH for H₂O. For DMSO, tetramethylammonium hydroxide from 1 molar solution in methanol was used to make 1 molar solution in anhydrous DMSO. The pK_a values were calculated using the BEST program.⁴¹

Table 8. pH values in H₂O for each template obtained from the potentiometric titration study.

0.1N NaOH (μ L)	Templates			
	1a	1b	1c	1d
0	3.2	3.32	3.04	3.14
20	3.42	3.47	3.19	3.29
40	3.51	3.63	3.34	3.44
60	3.67	3.74	3.49	3.58
80	3.8	3.89	3.65	3.71
100	3.93	4.05	3.81	3.84
120	4.08	4.16	3.99	3.97
140	4.25	4.42	4.2	4.1
160	4.47	4.54	4.42	4.23
180	4.79	4.78	4.64	4.37
200	5.54	5.19	4.85	4.51
220	6.52	5.68	5.05	4.65

240	6.87	5.96	5.24	4.79
260	7.09	6.18	5.44	4.94
280	7.25	6.36	5.66	5.07
300	7.42	6.52	5.96	5.21
320	7.57	6.67	6.38	5.34
340	7.73	6.81	6.86	5.5
360	7.88	6.98	7.2	5.67
380	8.07	7.16	7.43	5.88
400	8.29	7.38	7.64	6.2
420	8.59	7.7	7.84	6.83
440	8.96	8.29	8.06	8.34
460	9.48	9.14	8.31	9.22
480	10.03	9.86	8.67	9.64
500	10.19	10.26	9.3	9.89
520	10.42	10.48	10.0	10.06
540	10.6	10.46	10.4	10.2
560	10.72	10.56	10.6	10.28
580	10.71	10.67	10.7	10.37
600	10.8	10.75	10.8	10.45
620	10.86	10.82	10.8	10.53
640	10.92	10.88	10.9	10.6
660	10.96			10.66
680				10.72

Table 9. pH values in DMSO for each template obtained from the potentiometric titration study.

1 Molar $\text{Me}_4\text{N}^+\text{OH}^-$ (μL)	Templates			
	1a	1b	1c	1d
0	8.45	10.02	7.23	9.26
20	8.68	10.05	7.54	9.41
40	8.71	10.11	7.81	9.5
60	8.8	10.22	7.99	9.66
80	8.87	10.22	8.15	9.79
100	8.93	10.41	8.31	9.81
120	9.02	10.56	8.42	9.88
140	9.11	10.66	8.56	9.9
160	9.2	10.8	8.68	10.06
180	9.35	10.92	8.83	10.15
200	9.47	11.04	9	10.17
220	9.58	11.05	9.18	10.34
240	9.73	11.09	9.37	10.38
260	9.88	11.22	9.62	10.45
280	9.99	11.41	9.79	10.55
300	10.11	11.51	9.9	10.6
320	10.23	11.63	10.05	10.7
340	10.32	11.75	10.22	10.77
360	10.43	11.87	10.36	11.06
380	10.5	11.99	10.46	11.06
400	10.61	12.11	10.58	11.21

420	10.71	10.7	11.32
440	10.81	10.82	11.43
460	10.91	10.94	11.52
480	11.09	11.08	11.57
500	11.25	11.24	11.62
520	11.53	11.46	11.69
540	11.88	11.7	11.73
560	12.15	12.08	11.8
580	12.29	12.36	11.69
600	12.39	12.52	11.6
620	12.48	12.65	
640	12.58	12.75	

REFERENCES AND NOTES

- (1) Miller, S.; Janin, J.; Lesk, A. M.; Chothia, C. "Interior and surface of monomeric proteins." *J. Mol. Biol.* **1987**, *196*, 641-656.
- (2) A) Alber, S. D.; Baase, W. A.; Wozniak, J. A.; Matthews, B. W. "Structural and thermodynamic analysis of the packing of two α -helices in bacteriophage T4 lysozyme." *J. Mol. Biol.* **1991**, *221*, 647-667. B) Rashin, A. A.; Honig, B. "On the environment of ionizable group in globular proteins." *J. Mol. Biol.* **1984**, *173*, 515-521.
- (3) Gallivan, J. P.; Dougherty, D. A. "A computational study of cation-pi interactions vs salt bridges in aqueous media : implications for protein engineering." *J. Am. Chem. Soc.* **2000**, *122*, 870-874.
- (4) A) Dao-Pin, S.; Anderson, D. E.; Baase, W. A.; Dahlquist, F. W.; Matthews, B. W. "Structural and thermodynamic consequence of burying a charged residue within the hydrophobic core of T4 lysozyme." *Biochemistry* **1991**, *30*, 11521-11529. B) Dao-Pin, S.; Sauer, U.; Nicholson, H.; Matthews, B. W. "Contributions of engineered surface salt bridges to the stability of T4 lysozyme determined by directed mutagenesis." *Biochemistry* **1991**, *30*, 7142-7153.
- (5) Huyghues-Despointes, B. M. P.; Baldwin, R. L. "Ion-pair and charged hydrogen-bond interactions between histidine and aspartate in a peptide helix." *Biochemistry* **1997**, *36*, 1965-1970.

- (6) Lounnas, V.; Wade, R. C. "Exceptionally stable salt bridges in cytochrome P450cam have functional roles." *Biochemistry* **1997**, *36*, 5402-5417.
- (7) Schreiber, G.; Frisch, C.; Fersht, A. R. "The role of Glu73 of barnase in catalysis and the binding of barstar." *J. Mol. Biol.* **1997**, *270*, 111-122.
- (8) Schreiber, G.; Fersht, A. R. "Energetics of protein-protein interactions: Analysis of the barnase-barstar interface by single mutations and double mutant cycles." *J. Mol. Biol.* **1995**, *248*, 478-486.
- (9) Marqusee, S.; Sauer, R. T. "Contributions of a hydrogen bond / salt bridge network to the stability of secondary and tertiary structure in λ repressor." *Protein science* **1994**, *3*, 2217-2225.
- (10) Hendsch, Z. S.; Jonsson, T.; Sauer, R. T.; Tidor, B. "Protein stabilization by removal of unsatisfied polar groups: Computational approaches and experimental tests." *Biochemistry* **1996**, *35*, 7621-7625.
- (11) Kumar, S.; Nussinov, R. "Salt bridge stability in monomeric proteins." *J. Mol. Biol.* **1999**, *293*, 1241-1255.
- (12) Schneider, J. P.; Lear, J. D.; Kienker, P.K.; DeGrado, W. F. "Electrostatic effects on ion selectivity and rectification in designed ion channel peptides." *J. Am. Chem. Soc.* **1997**, *119*, 5742-5743.
- (13) Strop, p.; Mayo, S. L. "Contribution of surface salt bridges to protein stability." *Biochemistry* **2000**, *39*, 1251-1255.

- (14) Lounnas, V.; Wade, R. C. "Exceptionally stable salt bridges in cytochrome P450cam have functional role." *Biochemistry* **1997**, *36*, 5402-5417.
- (15) Albeck, S.; Unger, R.; Schreiber, G. "Evaluation of direct and cooperative contributions towards the strength of buried hydrogen bonds and salt bridges." *J. Mol. Biol.* **2000**, *298*, 503-520.
- (16) Honig, B. H.; Hubbell, W. L. "Stability of "salt bridges" in membrane protein." *Proc. Natl. Acad. Sci.* **1984**, *81*, 5412-5416.
- (17) Smith-Gill, S. J.; Wilson, A. C.; Potter, M.; Prager, E. M.; Feldmann, R. J.; Mainhart, C. R. "Mapping the antigenic epitope for a monoclonal-antibody against lysozyme." *J. Immunol.* **1982**, *128*, 314-322.
- (18) Somers, W.; Ultsch, M.; de Vos, A. M.; Kossiakoff, A. A. "The x-ray structure of a growth-hormone prolactin receptor complex." *Nature* **1994**, *372*, 478-481.
- (19) Spraggon, G.; Everse, S. J.; Doolittle, R. F. "Crystal structures of fragment D from human fibrinogen and its crosslinked counterpart from fibrin." *Nature* **1997**, *389*, 455-462.
- (20) Burley, S. k.; Petsko, G. A. "Amino-aromatic interactions in proteins." *FEBS Lett.* **1986**, *203*, 139-143.
- (21) A) Flocco, M. M.; Mowbray, S. L. "Planar stacking interactions of arginine and aromatic side-chains in protein." *J. Mol. Biol.* **1994**, *235*, 709-717. B) Ma, J. C.; Dougherty, D. A. "The cation-pi interaction." *Chem. Rev.* **1997**, *97*, 1303-1324.

- (22) Huebner, C. F.; Strachan, P. L.; Donoghue, E. M.; Cahoon, N.; Dorfman, L.; Margerison, R.; Wenkert, E. "Diels-Alder reaction of indene." *J. Org. Chem.* **1967**, *32*, 1126-1130.
- (23) Berson, J. A.; Aspelin, G. B. "On the mechanism of the indene-maleic anhydride reaction." *Tetrahedron* **1964**, *20*, 2697-2700.
- (24) Perumattam, J.; Shao, C.; Confer, W. L. "Studies on the alkylation and chlorination of fluorenes: preparation of 9-(2-hydroxyethyl)fluorene and 2,7-dichloro-9-(2-hydroxyethyl)fluorene." *Synthesis* **1994**, 1181-1184.
- (25) Kajigaeshi, S.; Kakinami, T.; Moriwaki, M.; Tanaka, T.; Fujisaki, S.; Okamoto, T. "Halogenation using quaternary ammonium polyhalides. XIV. Aromatic bromination and iodination of arenes by use of benzyltrimethylammonium polyhalides-zinc chloride system." *Bull. Chem. Soc. Jpn.* **1989**, *62*, 439-443.
- (26) Doyle, M. P.; Dellaria, J. F., Jr; Siegfried, B.; Bishop, S. W. "Reductive deamination of arylamines by alkyl nitrites in N,N-dimethylformamide. A direct conversion of arylamines to aromatic hydrocarbons." *J. Org. Chem.* **1977**, *42*(22), 3494-3498.
- (27) Otsuka, M.; Masuda, T.; Haupt, A.; Ohno, M.; Shiraki, T.; Sugiura, Y.; Maeda, K. "Man-designed bleomycin with altered sequence specificity in DNA cleavage." *J. Am. Chem. Soc.* **1990**, *112*, 838-845.
- (28) Hino, K.; Nakamura, H.; Shiro, Kato.; Irie, A.; Nagai, Y.; Uno, H. "Nonsteroidal anti-inflammatory agents. III. Synthesis of the metabolites of

- 10,11-dihydro-8, α -dimethyl-11-oxodibenz-[b,f]oxepin-2-acetic acid (bermoprofen)." *Chem. Pharm. Bull.* **1988**, *36(9)*, 3462-3467.
- (29) Furuta, K.; Iwanga, K.; Yamamoto, H. "Condensation of (-)-dimethyl succinate dianion with 1, ω -dihalides: (+)-(1S,2S)-cyclopropane-1,2-dicarboxylic acid." *Org. Synthesis* Vol. VIII, 141-145.
- (30) Saha, G.; Ghosh, S. "A new route to the synthesis of 7-functionalised bicyclo[2.2.1]heptane derivatives." *Synthetic Communications* **1991**, *21(21)*, 2129-2136.
- (31) Constantino, M. G.; Beatriz, A.; da Silva, G. V. J. "A model synthesis of the bicyclic core structure of the furanoheliangolde sesquiterpenes." *Tetrahedron Letters* **2000**, *41*, 7001-7004.
- (32) House, H.; Gall, M.; Olmstead, H. D. "The chemistry of carbanions. XIX. The alkylation of enolates from unsymmetrical ketones." *J. Org. Chem.* **1971**, *36(16)*, 2361-2371.
- (33) Konno, M.; Nakae, T.; Sakuyama, S.; Imaki, K.; Nakai, H.; Hamanaka, N. "An efficient method for the synthesis of a novel leukotriene B₄ receptor antagonist, ONO-4057, via Michael reaction of dihydroresorcinol." *Synlett.* **1977**, 1472-1474.
- (34) Corey, E. J.; Lazerwith, S. E. "A direct and efficient stereocontrolled synthetic route to the pseudopterosines, potent marine anti-inflammatory agents." *J. Am. Chem. Soc.* **1998**, *120*, 12777-12782.
- (35) Huffman, J. W.; Potnis, S. M.; Satish, A. V. "A silyl enol ether variation of the Robinson annulation." *J. Org. Chem.* **1985**, *50(22)*, 4266-4270.

- (36) Hayashi, M.; Inubushi, A.; Mukaiyama, T. "A convenient method for the preparation of secondary propargylic ethers. The reactions of acetals with 1-trimethylsilyl-1-alkynes promoted tin(IV) chloride and zinc chloride." *Bull. Chem. Soc. Jpn.* **1988**, *61*, 4037-.
- (37) Sato, T.; Wakahara, Y.; Otera, J.; Nozaki, H. "Oganotin triflate as practical catalyst for Michael addition of enol silyl ethers." *Tetrahedron* **1991**, *47*(47), 9773-9782.
- (38) A) Martell, A. E.; Motekaitis, R. J. "The determination and use of stability constants"; VCH: New York, 1988. B) Ishida, T.; Ohnishi, K.; Dot, M.; Inoue, M. "Proton nuclear magnetic resonance study on the aromatic amino acid-guanine nucleotide system: effect of base methylation on the stacking interaction with tyrosine and phenylalanine." *Chem. Pharm. Bull.* **1989**, *37*, 1-4.
- (39) Kamiichi, K.; Doi, M.; Nabaie, M.; Ishida, T.; Inoue, M. "Structural studies of the interaction between indole derivatives and biologically important aromatic compounds. Part 19. Effect of base methylation on the ring-stacking interaction between tryptophan and guanine derivatives: a nuclear magnetic resonance investigation." *J. Chem. Soc. Perkin. Trans. II* **1987**, 1739-1745.

(40) Phosphate buffer

pH	Solution A (mL)	Solution B (mL)
	0.1M NaH ₂ PO ₄	0.1M Na ₂ HPO ₄
7	39	61
7.5	16	84
7.6	13	87
7.8	8.5	91.5
8	5.3	94.7
8.5	2	98

(41) A) Gustowski, D. A.; Gatto, V. J.; Mallen, J.; Echevoyen, L.; Gokel, G. W. "Direct correlation of cation binding strengths to Hammett parameters in substituted N-benzylaza-15-crown-5 lariat ether and N,N'-dibenzyl-4,13-diaza-18-crown-6 BiBLE derivatives." *J. Org. Chem.* **1987**, *52*, 5172-5176.

B) Taft, R. W. *J. Phys. Chem.* **1960**, *64*, 1805-. B) Gross, K. C.; Seybold, P. G. "Comparison of quantum chemical parameters and Hammett constants in correlating pK_a values of substituted anilines." *J. Org. Chem.* **2001**, *66*, 6919-6925.

(42) A) Thomas, P. D.; Podder, S. K. "Specificity in protein – nucleic acid interaction." *Febs Letters.* **1978**, *96*, 90-94. B) Modi, S.; Behere, D. V.; Mitra, S. "Binding of aromatic donor molecules to lactoperoxidase : proton NMR and optical difference spectroscopic studies." *Biochimica et Biophysica Acta.* **1989**, *996*, 214-225.

